Engineering Failure Analysis 131 (2022) 105845

Contents lists available at ScienceDirect

Engineering Failure Analysis

journal homepage: www.elsevier.com/locate/engfailanal

Performance assessment of deteriorating reinforced concrete drainage culverts: A case study

Yao Tang [a,*], Yuequan Bao [b], Zhi Zheng [c], Jie Zhang [d], Yongchang Cai [e]

[a] Key Laboratory of Geotechnical and Underground Engineering of Ministry of Education and Department of Geotechnical Engineering, Tongji University, Shanghai 200092, China
[b] Shanghai Chengtou Water Group Co. Ltd., Shanghai 201103, China
[c] Poly Bay Area Investment and Development Co. Ltd., Dongguan 523000, China
[d] Key Laboratory of Geotechnical and Underground Engineering of Ministry of Education and Department of Geotechnical Engineering, Tongji University, Shanghai 200092, China
[e] Key Laboratory of Geotechnical and Underground Engineering of Ministry of Education and Department of Geotechnical Engineering, Tongji University, Shanghai 200092, China

A R T I C L E I N F O

Keywords:
Corrosion
Drainage culverts
Reinforced concrete
Gamma process
Failure probability

A B S T R A C T

Rectangular reinforced concrete (RC) culverts are widely used in drainage systems of many megacities, which may experience significant deterioration due to the corrosive sewage environment. How to assess the performance of existing RC culverts is crucial to the public safety. Currently, very few studies have been reported on the assessment of the performance of deteriorating RC culverts which are in service. This paper reports the research work on the performance assessment of a drainage culvert in Shanghai, China, which is one of the most populous megacities in the world. Field investigations are first conducted to examine the deterioration of drainage culverts in the real world. The deterioration of the culvert is modeled through a stochastic model, which is calibrated based on field investigation data. The performance of the culvert is then examined through the local design code, which seems to be overconservative for ultimate bearing capacity assessment. To avoid the conservative assumptions in the design code method, a high-resolution finite element model is built to assess the performance of the culvert. During the assessment process, the uncertainty associated with the deterioration is also considered. Based on the findings from the research, recommendations are made regarding the maintenance of the drainage culverts. The research reported in this paper may also provide useful reference for assessing the performance of deteriorating culverts in other regions of the world.

1. Introduction

Owing to the highly corrosive service environment, the deterioration of the reinforced concrete (RC) drainage culvert is fast and severe, which may make to its actual service life far less than the design life [1–3]. In recent decades, accidents such as sewage overflow and road collapse caused by the aging of drainage systems have been widely reported worldwide, such as the Coxwell pipeline crisis in Toronto, Canada [4], and the downtown sewer collapse in Louisville, America [5]. The structural deterioration of drainage systems and

* Corresponding author.
E-mail addresses: 1610132@tongji.edu.cn (Y. Tang), zhengzhi@polycn.com (Z. Zheng), cezhangjie@tongji.edu.cn (J. Zhang), yccai@tongji.edu.cn (Y. Cai).

https://doi.org/10.1016/j.engfailanal.2021.105845
Received 14 July 2021; Received in revised form 13 October 2021; Accepted 29 October 2021
Available online 1 November 2021
1350-6307/

their subsequent failures can entail critical consequences for society and industry [6,7]. To manage the risk posed by deteriorating RC drainage culverts, assessment of the performance of deteriorating RC drainage culverts is very important.

Over the past few decades, many studies have been conducted on the corrosion mechanism of RC drainage culverts [8–10]. It has been widely recognized that the service environment of drainage culverts contains a variety of physical, chemical, and biological corrosion sources. Specifically, the physical corrosion typically includes the erosive wear caused by the sewage flow, the shrinkage and swelling of concrete caused by the drying-wetting cycle. The biological corrosion is derived from sulfide bacteria, nitrifying bacteria, fungi, and other microorganisms, which can rapidly reduce the PH on pipes' inner surface and then neutralize and soften the concrete [11]. The corrosive solute and acid escaping gas (such as H_2S) react on the concrete surface and generate sulfuric acid, further eroding the culverts [10]. The sewage can also provide a conductive solution for electrochemical corrosion and accelerate the rusting of steel bars [12].

Several studies have also been conducted to assess the corrosion rate of drainage culverts. For example, EPAT [13] suggested a semi-empirical model to predict the corrosion rate of concrete considering the effects of concentration of H_2S and PH, but the specific value of the corrosion factor k lacks in research. Herisson et al. [8] and Jiang at al. [9] reported that the corrosion rate of drainage culverts is affected by many factors, including the concentration of H_2S, temperature, humidity, and the PH of the service environment. Wells and Melchers [14] found that the corrosion rate of drainage culverts was most closely related to H_2S concentration and suggested a corrosion rate prediction model. While these studies provided useful insight on the mechanism of the deterioration of RC drainage culverts, the deterioration models developed were mainly based on tests conducted in the well-controlled laboratory environment. Very few studies have been reported on how to assess the performance of RC drainage culverts in the real world.

Shanghai, which has a population of 24 million, is the most populous city in China, and is also one of the largest cities in the world. The drainage network in Shanghai's central urban district consists of several arterial drainage culverts built in succession since the 1970s. By 2015, the total drainage pipelines in Shanghai were about 13319 km, among which the total length of extra-large reinforced concrete drainage culverts (with inner diameter greater than 1.5 m) is about 900 km. The focus of this study is the Shanghai Nangan Line, which is an important branch line of the extra-large reinforced concrete drainage line, and it was complete in 1984. Currently, the Nangan line provides sewage transportation service for about 1.3 million residents, with a daily volume of sewage of about 300,000–400,00 m^3. After operation for more than three decades, the ceiling of the drainage culvert was found to be seriously eroded and even several sewage leakage was observed in several sections [15]. There is an increasing concern regarding the real performance of the RC drainage culverts along this line with focus on the following questions. Firstly, what is the corrosion rate of the RC drainage culvert along the Nangan line? Secondly, does its structural performance still meets the design specifications? Thirdly, if the answer to the second question is no, what is its residual life of the drainage culvert? While the deterioration of drainage culverts has been widely noticed worldwide, very few studies have been reported in the literature regarding the performance of deteriorating drainage culverts in the real world.

The objective of this case study is to report the research work conducted in Shanghai to answer the above questions, which was initiated in 2014. This paper is organized as follows. First, the field investigation results regarding the Nangan line are introduced. Then, a stochastic deterioration model is established to predict the corrosion of the drainage culvert. Thereafter, the performance of the drainage culvert is assessed through the local design code, where the structural forces are calculated based on the moment distribution method and the structural resistance is calculated through the limited stated method. Finally, the performance of the drainage culvert is assessed through the finite element method (FEM) model, where longitudinal bars on the compression side can be considered. The effect of uncertainties on the assessment of performance of the deteriorating drainage culverts is also discussed. The research findings reported in this paper may provide useful references for how to assess the performance of deteriorating RC drainage culverts in the real word in other parts of the world.

Fig. 1. Excavation site of the Shanghai Nangan Line.

2. Field investigation

The Shanghai Nangan Line studied in this paper is a box-shaped sewer pipe with a width of 3200–3700 mm, a height of 2500 m, and a thickness of 250 mm. To understand the actual deterioration status of the culverts, a series of field investigations were conducted in 2014. As an example, Fig. 1 shows the excavation site of an inspected section. During the field inspection, the distribution and the residual cross-sectional area of steel bars, the residual thickness of the concrete and the compressive strength of concrete were carefully examined. For the roof of the drainage culverts, it is found that quite some longitudinal bars disappeared, and the thickness of the corroded concrete was generally between 40 and 90 mm. In addition, the concrete strength is grade C30 according to the test results of the drilling core samples, which means that the change of material properties of concrete was not obvious. Through the field investigation, it is found that while the ceiling is seriously eroded, the structure under the water is almost intact. The possible reason is that H_2S in sewage escapes upward and accumulates at the top, which eventually turns into sulfuric acid. However, thanks to the long-term hypoxia under the water, the dissolved oxygen is not enough to support the oxidation of sulfide ions. The chemical reaction of weak acid to strong acid cannot occur although sulfide bacteria exists. Similar phenomenon was also observed in U. K. about the corrosion of standard gravity flow pipelines in the above sewage environment under the non-full operating condition [16]. To simplify the analysis process and facilitate engineering application, the concrete loss and reinforcement loss under different service conditions were mainly considered in the calculation in this paper, while the change of the material properties with time is ignored.

As an example, Fig. 2 shows the CCTV pictures of the roofs taken from the inner side of the culverts, and Table 1 summarized the

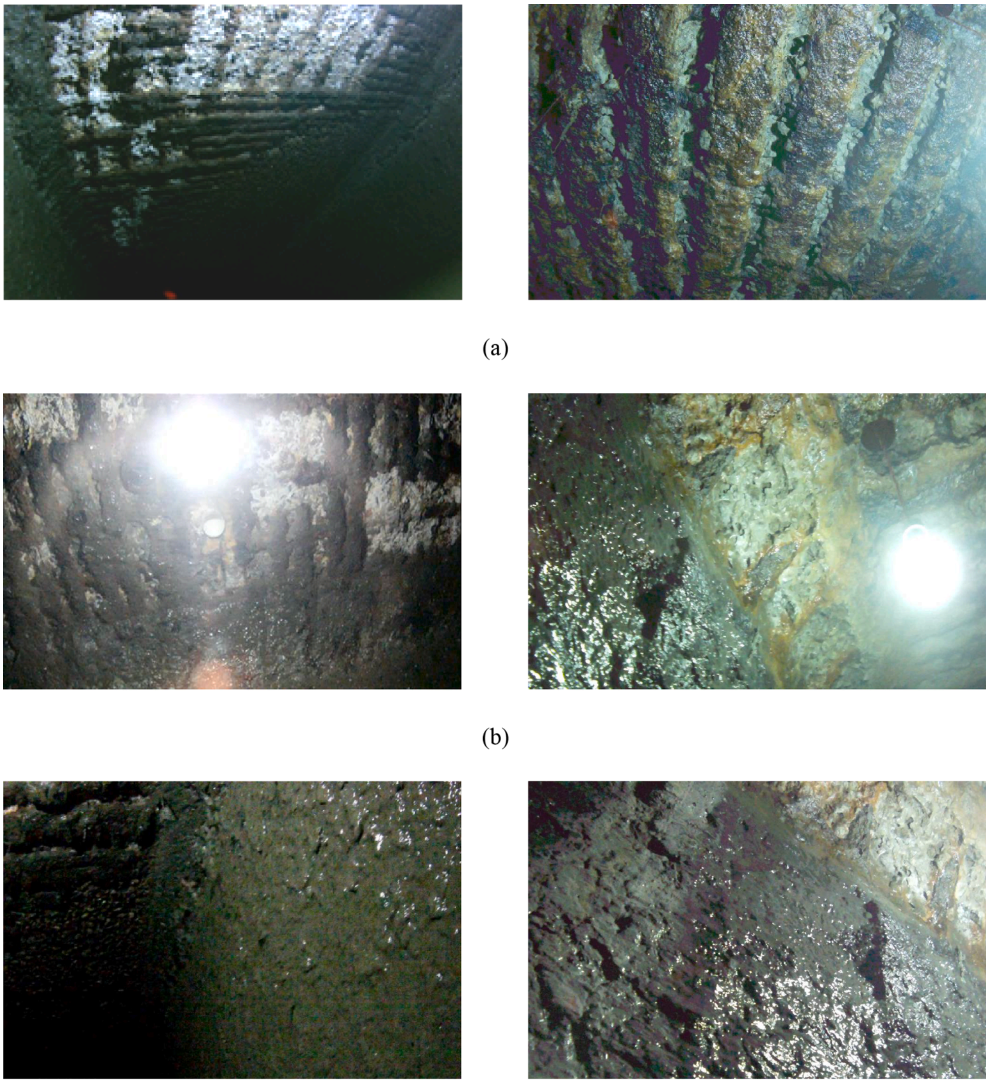

(a)

(b)

(c)

Fig. 2. CCTV pictures of the Shanghai Drainage Line: (a) Roof; (b) Haunch; (c) Sidewall.

Table 1
Measured value of concrete corrosion thickness.

Section number	1	2	3	4	5	6
Service time (year)	32	32	32	34	34	35
Corrosion thickness of concrete (mm)	60	30	80	90	60	70

maximum thickness of the corroded concrete measured at the roof of the culverts at six typical cross sections. Based on the above observations, Fig. 3 shows the corrosion condition of a typical cross section of the drainage culvert in the Nangan line, which will be used to develop the computational model to analyze the performance of the drainage culverts.

3. Deterioration model

As mentioned previously, although many laboratory studies have been conducted on the deterioration of RC drainage culverts, it is not straightforward to apply such models in the real world as the input parameters for such models in the real world are hard to determine. To consider the uncertainty of the real-world corrosion process, the Gamma process, which is a stochastic model widely used for modeling the degradation process of structures [17–19] is adopted in this paper to analyze the deterioration of the RC drainage culvert.

In the Gamma process model, let the random process $x(t)$ denote the corroded thickness of the concrete at time t. Assuming that at time t (year) the corroded thickness follows the Gamma distribution with a shape parameter of $\alpha(t) > 0$ and a scale parameter of $\beta > 0$, its probability density function (PDF) can be written as follows:

$$f[(x(t)|\alpha(t),\beta)] = \frac{\beta^{\alpha}}{\Gamma(\alpha)}x^{\alpha-1}\mathrm{e}^{-\beta x} \tag{1}$$

where $\Gamma(\alpha) = \int_{z=0}^{\infty} z^{\alpha-1}\mathrm{e}^{z}dz(\alpha > 0)$ is the Gamma function. Based on the property of a Gamma distribution, it can be shown that the mean and the variance of corroded thickness of the concrete at time t can be written as follows.

$$\mathrm{E}[x(t)] = \frac{\alpha(t)}{\beta} \tag{2}$$

$$\mathrm{Var}[x(t)] = \frac{\alpha(t)}{\beta^2} \tag{3}$$

For typical structural degradation, the shape parameter can be often modeled with a time-dependent power function as follows [20]:

$$\alpha(t) = c \cdot t^{b} \tag{4}$$

where c and b are corrosion constants, which can be calibrated by measured values. For sulfide attacks, Ellingwood and Mori [21]

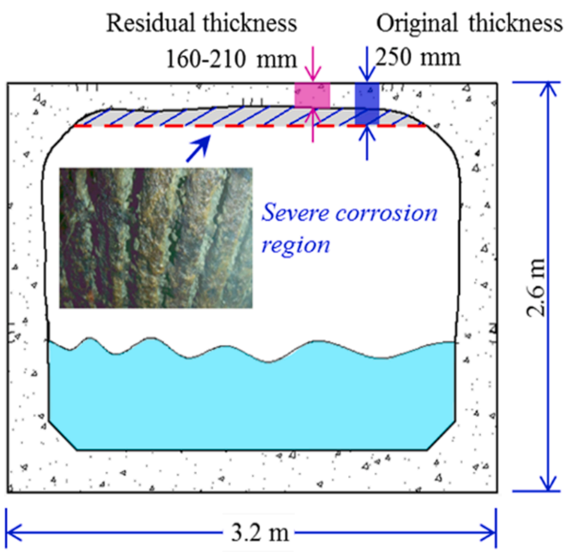

Fig. 3. Simplified illustration of the corrosion condition [15].

recommended $b = 2$. In this paper, $b = 2$ is adopted.

After the value of b is determined, there are two remaining parameters in the Gamma process model, i.e., c and β. Suppose there are n observations regarding the corroded thickness of the drainage culverts. Let δ_i denotes observed corroded thickness at time t_i . Suppose when the values of c and β are knows, the observed corroded thickness at different times are statistically independent. The likelihood function of c and β, i.e., the chance to observe $\delta_i(i = 1, 2, \cdots, n)$, can then be written as follows.

$$l(\delta_1, \delta_2, \cdots, \delta_n | c, \beta) = \prod_{i=1}^{n} \frac{\beta^{c \cdot t_i^b}}{\int_{z=0}^{\infty} z^{c \cdot t_i^b - 1} e^z dz} \delta_i^{c \cdot t_i^b - 1} e^{-\beta \delta_i} \tag{5}$$

Based on the maximum likelihood principle, the optimal values of c and β can be obtained by maximizing Eq. (5), or equivalently, the logarithm of Eq. (5), which yields $c = 0.01$ and $\beta = 0.17$.

Based on the above calibrated model, Fig. 4 displays the PDF of corrosion thickness of the roof as the service time changes. It can be seen from the figure that the width of the PDF increases with service time, which indicates that the uncertainty of corrosion thickness of the drainage culvert increases. Based on Eq. (2), Fig. 5 shows the relationship between the mean of the corrosion thickness of concrete in the roof and service time. Fig. 5 indicates that the corrosion thickness is almost zero in the first few years of service, and the corrosion rate increases with time. When the service time is 32 years, the mean value of the corrosion thickness is 60 mm.

In the above analysis, the deterioration model of the concrete is established. To analyze the performance of the drainage culvert, the deterioration model of the steel bars should also be established. In this study, the corrosion of steel bars refers to the corrosion of the longitudinal bars on the tension side, and the corrosion of the longitudinal bars on the compression side is ignored because of less contact with the corrosion source. It is assumed that the longitudinal bars are intact before the corrosion depth reaches 30 mm, i.e., thickness of the concrete over, and the longitudinal bars disappears when the corrosion depth reaches 42 mm, i.e., the sum of the concrete cover thickness and the diameter of the steel bar. When the corrosion thickness is between 30 mm and 42 mm, the cross-sectional area of the steel bars decreases linearly with the corrosion thickness of the concrete. In addition, the change of the strength of the steel bars is not considered. In reality, the deterioration of the steel bars is affected by various complex factors such as the combined interaction between passivation of layers, chemical action, the non-ideal Fick diffusion and t [22,23]. The corrosion of steel bars could be more complex than the assumptions as described above. However, very few studies have been made on the deterioration of steel bars in the drainage culverts. In addition, as will be seen from the analysis described in later of this paper and the structural failure of the drainage culvert occurs after the steel bars are fully corroded. To simplify the analysis of the drainage culvert, the simplified assumptions regarding the deterioration of the steel bars are adopted.

4. Performance assessment based on design code

To assess the performance of the deteriorating RC drainage culvert, a typical cross section of the Shanghai Nangan Line is considered, as shown in Fig. 6. As illustrated in this figure, there are three layers of soil involved in this section: fill soil, silty clay, and mucky silty clay. In Shanghai, the drainage culvert is designed based on CECS [24], and Fig. 7 shows the force diagram specified in CECS [24]. Based on the code, the performance of the drainage culverts should be checked under two design scenarios, i.e., the scenario where the drainage culvert is empty while the groundwater level is high (Scenario I), and the scenario where the drainage culvert is full and the groundwater level is low (Scenario II). The calculation equations and results of loads are displayed in Table 2, the supplementary notes of the selection of calculation parameters and load combination in Table 2 are in Appendix A.

Based on the loads calculated in Table 2 and the force diagram in Fig. 7, the bending moment of the typical cross section under two design scenarios is calculated through the moment distribution method specified in CECS [24]. As an example, Fig. 8(a) and (c) show the bending moment diagrams of the drainage culvert under design scenario I when the corrosion depth is 0 and 36 mm, i.e., the tensile reinforcement area is deduced to 50%, respectively.

Assuming that the tensile strength of the concrete and the steel bars on the compression side is zero, when the longitudinal bars on the tension side works, the flexural capacity of the roof can be calculated as follows based on Chinese code for design of concrete structures [25]:

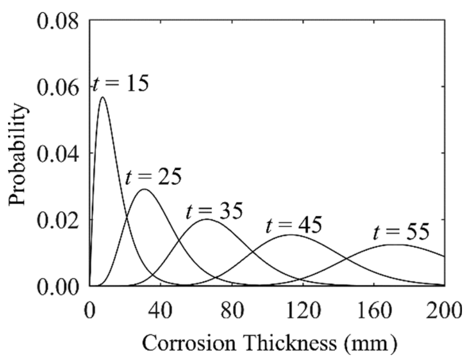

Fig. 4. Probability distribution of corrosion thickness.

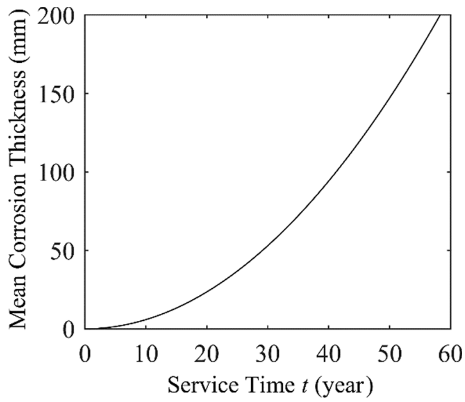

Fig. 5. Relationship between corrosion thickness and service time.

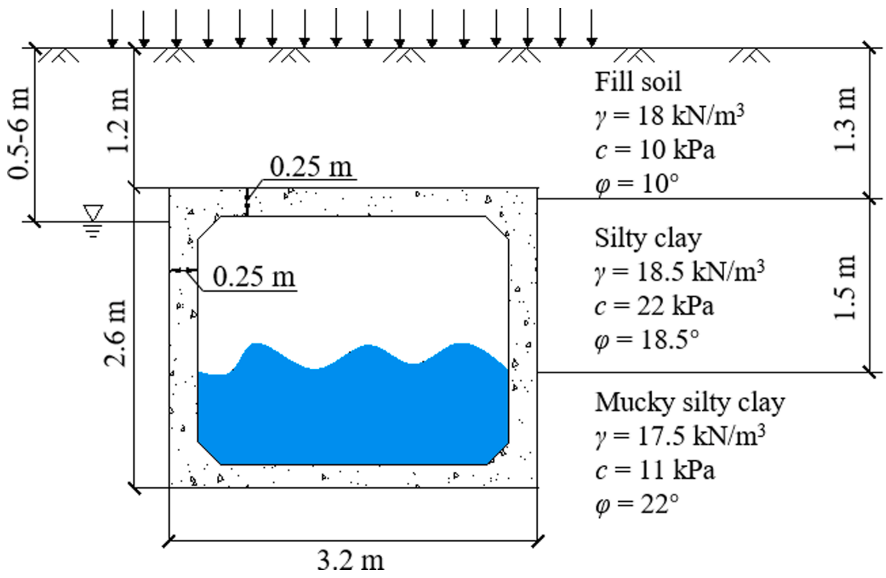

Fig. 6. Illustration of the typical section.

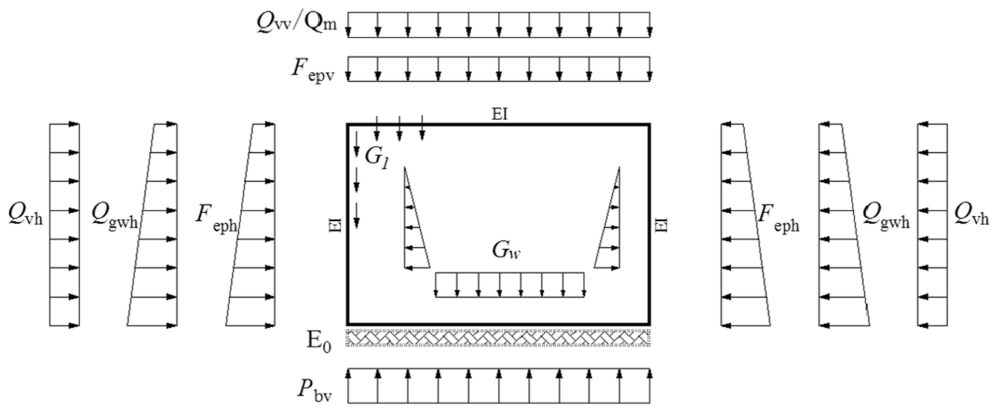

Fig. 7. The force diagram of drainage culverts.

$$M_u = f_y \cdot A_s \cdot h_0 \left(1 - \frac{a_s}{h_0}\right) \tag{6}$$

Table 2
Load calculation equations and results

Load	Formula	Symbol	High water level	Low water level	Unit
Gravity	$\gamma_c \cdot b \cdot h$	$G_{I,k}$	6.25	6.25	kPa
Water pressure inside	$\gamma_w(Z - Z_{top} - h)$	$G_{w,k}$	[0, 21]	[0, 21]	
Vertical earth pressure	$C_d \cdot \gamma_s \cdot Z_{top} \cdot b$	$F_{epv,k}$	25.92	25.92	
Active earth pressure	$K_a \cdot [\gamma_s \cdot Z_w + \gamma_s^{'} \cdot (Z - Z_w)]$	$F_{eph,k}$	[5.33, 14]	[7.2, 22.8]	
Water pressure outside	$\gamma_w \cdot (Z - Z_w)$	$Q_{gwh,k}$	[7,33]	[0,0]	
Variable load	Take the most adverse value	Q_{vv}/Q_m	10	10	
Foundation reaction	$N_s/(b \cdot l)$	P_{bv}	48.42	69.42	

Note: [a, b] means that the load at the top of the sidewall is a (kPa), and the load at the bottom is b (kPa), and the load changes linearly between a and b.

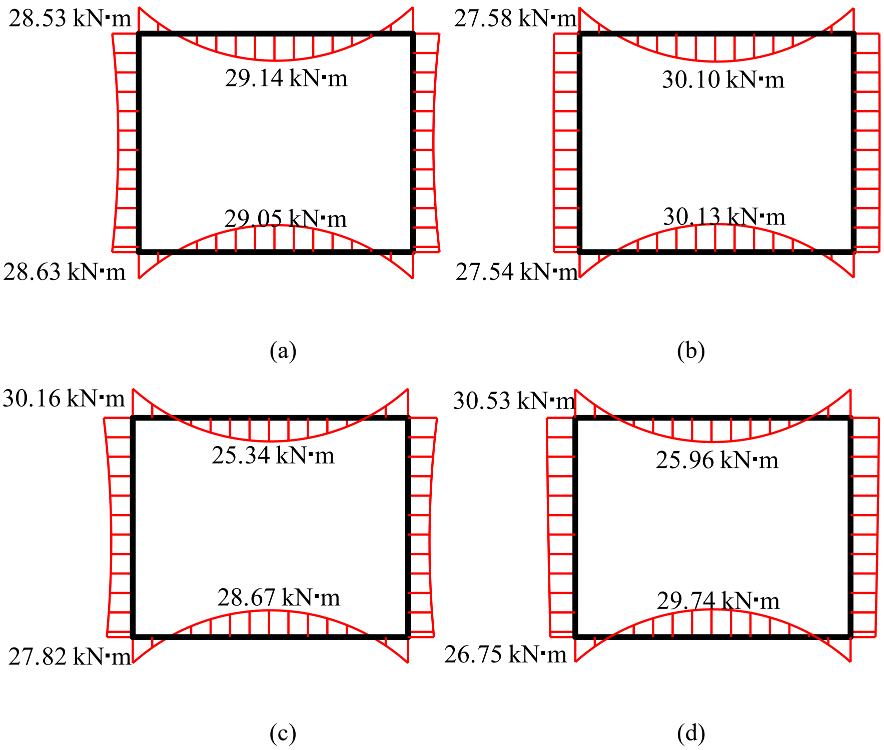

Fig. 8. Bending moment diagrams: (a) Scenario I (corrosion thickness is 0 mm); (b) Scenario II (corrosion thickness is 0 mm); (c) Scenario I (corrosion thickness is 36 mm); (d) Scenario II (corrosion thickness is 36 mm).

where the tensile strength of steel bars f_y is 300 MPa, A_s is the cross sectional area of the steel bars on the tension side, h_0 is the effective height of the section and a_s is the distance between resultant point of steel bars and tensile edge of the section.

When the longitudinal bars on the tension side disappear, the flexural capacity is calculated as follows:

$$M_u = \gamma \cdot f_{ct} \cdot \frac{b \cdot h^2}{6} \tag{7}$$

$$\gamma = \left(0.7 + \frac{120}{h}\right)\gamma_m \tag{8}$$

$$f_{ct} = 0.55 f_t \tag{9}$$

where γ is the plastic influence coefficient of concrete under bending moment, $\gamma_m = 1.55$ is the basic value of the plastic influence coefficient of concrete under bending moment, f_{ct} is the design value of axial tensile strength of plain concrete, and h is 400 mm for this cross section. The tensile strength of concrete f_t is 1.43 MPa. The section thickness t is 250 mm and the calculation length b is 1 m.

When there is no corrosion, the maximum bending moment of the roof is located in the mid-span. As the corrosion develops, the position of the maximum bending moment transfers to the haunches. However, although the bending moment in the mid-span of the roof after corrosion is less than the haunches, the corrosion only reduces the flexural capacity of the mid-span of the roof. Therefore, the factor of safety (FOS) of both sections is calculated, and the smaller value is taken as the value of the FOS.

Fig. 9 shows the relationship between the FOS of the roof against bending and the corrosion thickness. As can be seen from this figure, the FOS first increases slightly during the initial period of corrosion. At this stage, the bending moment of the roof decreases with stiffness due to corrosion, while the calculated flexural capacity at the mid-span of the roof is not changed because the tensile strength of concrete is not considered in the Eq. (5) and Eq. (6). As the corroded thickness further increases, the most critical section changes to the haunches, which leads to a trend of decreasing FOS with the increase of the corrosion thickness. After the corrosion thickness reaches the steel bars, the most critical section returns to the mid-span and in such a case the FOS of the culvert decreases rapidly with the corrosion thickness. The FOS of the culvert decreases from 2.25 to 1.0 when the reinforcement area decreases from its initial value to half (with the corrosion thickness of 36 mm).

Taking the mean corrosion thickness as calculated by Eq. (2) as the input, the FOS of the drainage culvert at different service time can then be calculated. Based on the first order second moment method [26], the FOS of the drainage culvert calculated in such a way can be regarded as the mean of the FOS of the drainage culvert considering the uncertain corrosion thickness. Fig. 10 shows the relationship between the mean FOS of the drainage culvert and the service time. As can be seen from this figure, when the service time is 25 years, the FOS of the drainage culvert drops to 1.0, indicating the service life is 25 years based on the FOS of the drainage culvert.

In the above analysis, the mean FOS of the culvert is analyzed. In reality, at a given service time the corrosion thickness is uncertain and hence the FOS of the culvert is also uncertain. In such a case, the performance of the culvert may be measured thought the failure probability, which can be defined as the probability that the FOS of the culverts is less than 1.0. As mentioned above, the FOS of the culvert is 1.0 when the corrosion thickness is 36 mm. As such, the failure probability of the culvert at time t can be calculated as the probability that the corrosion thickness is greater than 36 mm at such a time. Fig. 10 also shows the variation of the failure probability with time. As shown in this figure, in the first 13 years of service, the failure probability of the structure is less than 1 %. After 13 years of service, the failure probability of the drainage culvert will start to increase rapidly. When the service time is 35 years, the failure probability of the culvert is nearly 100%, indicating it is almost sure that the drainage culvert will failure at the age of 35 years old.

Based on the above analyses, it seems that the service life of the drainage culvert is no more than 35 years. Such a conclusion, however, seems to contradict with the reality that while sewage leakages has been occasionally observed in Shanghai, widespread failure of the drainage culverts has not yet been observed up to now, which has a service time of 37 years in the year of 2021. Such a contradiction may be caused by the simplified assumptions involved in the evaluating the FOS of culvert. As mentioned previously, in Eq. (6) and Eq. (7), the longitudinal bars on the compression side is not considered. This conservative assumption may have significant impact on the FOS of the drainage culvert. To assess the performance of the culvert more realistically, the performance of the culvert will be analyzed based on FEM, as described in the following section.

5. Performance assessment of the drainage culvert based on FEM

To overcome the limitations of the design code method, the performance of the drainage culvert will be analyzed through a finite element model built in ABAQUS [27] in this study, which can simulate the ultimate bearing capacity of the degenerated RC drainage culvert considering the tensile strength of the longitudinal bars on both sides of the roof as well as the tensile strength and post-peak softening behavior of concrete.

5.1. Finite element model

5.1.1. Constitutive relationship for materials

Reinforcement. The tri-linear elastic-plastic model [28] considering the hardening behavior of reinforcement is applied in simulation. The yield stress f_y , the elastic modulus E_s and Poisson's ratio ν are taken in the light of the code [25], and the flow amplitude ε_f is approximately 1% in consonance with the data of the strain gauges in the full-scale tests [29]. The parameters of the tri-linear elastic-

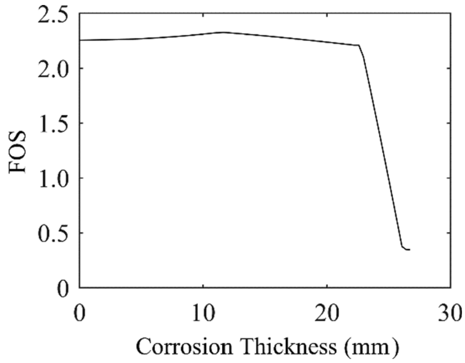

Fig. 9. Relationship between mean FOS and corrosion thickness.

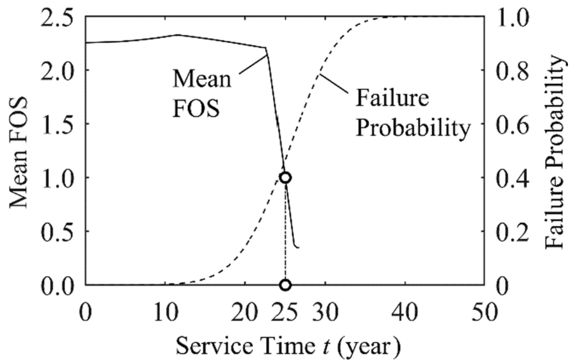

Fig. 10. Relationship of FOS and failure probability with time.

plastic model are summarized in Table 3.

Concrete. On the strength of the work of Lubliner et al. [30], Lee and Fenves [31], a concrete damaged plasticity (CDP) model was set up to consider damage and plasticity simultaneously, which has been embedded in the commercial FEM program ABAQUS and was employed to simulate concrete in this research. In the CDP model, besides the basic parameters such as density, elastic modulus and Poisson's ratio, the plastic parameters of the material and the constitutive curve need to be defined. The density γ, elastic modulus, E_c and Poisson's ratio ν are taken in accordance with MOHURD [25]. The plastic parameters: ratio biaxial to uniaxial compressive strength f_{bc}, dilation angleψ, parameter of the flow potential G second stress invariant ratio K_c , eccentricity $\in$, and viscosity parameter μ are taken in accordance with DSSC [27] and relevant literatures [30–32]. The basic elastic and plastic parameters are summarized in Table 4. The uniaxial compressive stress–strain relationship is determined based on MOHURD [25], and the stress–strain relationship is calculated as follows:

$$\sigma = (1 - d_c) \cdot E_c \cdot \in, \quad \text{with} \ \ d_c = \begin{cases} 1 - \dfrac{\rho_c \cdot n}{n - 1 + x^n}, x \le 1 \\ 1 - \dfrac{\rho_c}{\alpha_c (x-1)^2 + x}, x > 1 \end{cases} \tag{10}$$

$$\rho_c = \frac{f_{c,r}}{E_c \varepsilon_{c,r}} \tag{11}$$

$$n = \frac{E_c \varepsilon_{c,r}}{E_c \varepsilon_{c,r} - f_{c,r}} \tag{12}$$

$$x = \frac{\varepsilon}{\varepsilon_{c,r}} \tag{13}$$

where d_c is the uniaxial compression damage parameter, $f_{c,r}$ is the representative value of uniaxial compressive strength of concrete, the parameter of the descending section of the constitutive curve $\alpha_c = 0.74$, and the peak compressive strain corresponding to the uniaxial compressive strength $\varepsilon_{c,r} = 0.00147$.

The ascending part of the tension curve is considered as ideal linear elastic, and the softening part is a fracture-energy-based exponential curve [33]:

$$\frac{\sigma(w)}{f_t} = \left[1 + \left(c_1 \cdot \frac{w}{w_c}\right)^3\right] \cdot exp\left(-c_2 \cdot \frac{w}{w_c}\right) - \frac{w}{w_c} \cdot (1 + c_1^3) \cdot exp(-c_2) \tag{14}$$

$$w_c = \frac{5.14 G_f}{f_t} \tag{15}$$

where w is the crack opening, w_c is the critical crack opening, the fracture energy G_F has a value of 100 J/m^2 and $c_1 = 3, c_2 = 6.93$ [33].

In addition to the above parameters, in the CDP model, a single damage variable D is used to reflect the degradation of unloading

Table 3
Mechanical properties of steel bars

Type (HRB)	Elastic parameter			Plastic parameter		Strength parameter	
	γ (kN/m^3)	E_s (GPa)	ν	ε_f	ε_u	f_y (MPa)	r_{yu}
335	78	200	0.3	1%	4%	300	0.8

Table 4
Mechanical properties of concrete

Grade	Elastic parameter			Plastic parameter					Strength parameter	
	γ (kN/m^3)	E_c (MPa)	ν	K_c	f_{bc}	ψ (°)	ϵ	μ	f_t (MPa)	G_f (N/m)
C30	24	30,000	0.2	0.67	1.16	30	0.1	0.001	2.01	100

stiffness caused by irreversible microcracks. The D is determined through the Birtel fixed plastic strain ratio method [32].

The results of the full-scale experiments indicate that the contact between reinforcement and concrete has little effect on the bearing capacity and ultimate deformation of the structure [29]. Hence, reinforcement and concrete are modeled separately, and the bond-slip is neglected. The reinforcement was modeled as the embedded region in concrete using constraints in the interaction module and making the concrete the host.

5.1.2. Load and boundary conditions

The load-structure model is used in this paper. The bottom and two sides of the drainage culvert are constrained by soil springs that can only withstand compressive stress, and the ends of the springs away from the culvert are fixed. The stiffness of the soil springs is determined by the m-method [34], where the proportionality coefficient m is taken as 5 MN/m^4 in the simulation based on the properties of the soil, and the corresponding foundation coefficient $K_v = 50000$ kN/m^3. Line loads on the top and two sides of the structure are applied as shown in Fig. 7, the specific values are obtained from Table 2.

5.1.3. Mesh of the FEM model

Fig. 11 shows the mesh of the FEM model. In the FEM model, the global mesh size is 25 mm, and the meshing strategy is quad-dominated. For the concrete, the elements are 4-node bilinear plane strain quadrilateral, reduced integration, hourglass control (CPE4R), and 3-node linear plane strain triangle (CPE3). For the steel bar, the elements are 2-node linear 2-D truss (T2D2truss).

Since the centralized softening during the calculation results in that the cracking process relies on the meshing, the influence of mesh size is taken into account in the definition of the stress–strain curve of concrete. Specifically, based on the stress-crack width curve and mesh size, the strain calculated through the formula below can be converted into a stress–strain curve:

$$\varepsilon = w/l_{ch} \tag{16}$$

where w is the crack width, l_{ch} is the characteristic length of the element [35].

In the FEM model, the mesh should be uniform as much as possible, and its size is approximately taken as global mesh seed interval. In this paper, the uniform global mesh size of 25 mm is used as the element characteristic length l_{ch} .

The model in the simulation were verified by the full scale tests [29]. Taking the mid-span deflection of the roof under the standard load as the reference index, the drainage culvert in different corrosion states is simulated. The ultimate life is analyzed according to the curve obtained.

5.2. Impact of corrosion on the service of drainage culverts

Fig. 12 shows the relationship between the mid-span deflection of the roof and the corrosion thickness. As can be seen from this figure, before the corrosion thickness reaches 130 mm, the mid-span deflection is almost the same as the initial value, which is 2–3 mm. As the corrosion develops, the deflection increases slowly to about 15 mm. When the corrosion thickness is greater than 170 mm, the deflection increases rapidly, indicating that the structure can no longer bear the load. Eventually, three plastic hinges appear in the mid-span and two ends of the roof, resulting in the failure of the structure. Fig. 13 shows the strain diagram when the structure is destroyed.

Using the mean corrosion thickness as calculated by Eq. (2) as the input, the computed deflection can be regarded as the mean deflection of the roof based on the first order second moment method [26]. Fig. 14 shows the relationship between the mean deflection of the roof of the culvert and the service time. As can be seen from this figure, when the service time is about 54 years, the mean deflection of the roof is about 15 mm and starts to increase dramatically. If we regard the mean corrosion thickness of 170 mm as the allowable deflection, the service life is about 54 years. To consider the effect of uncertainty in the corrosion thickness, Fig. 14 also shows how the failure probability of the culvert changes with time, where the failure probability is defined as the probability that the corrosion thickness is greater than 170 mm. As can be seen from this figure, the failure probability of the structure is less than 1% during the first 42 years of service, indicating that when the age of the drainage culvert is less than 42 years, the chance to observe structural failure is very small. That is largely consistent with the current observation, that no structural failure of the drainage culvert has been observed up to now. Fig. 14, however, also shows that, after 42 years of service, the failure probability of the drainage culvert will start to increase rapidly. When the service time is 65 years, the failure probability of the culvert is nearly 100%, indicating it is almost sure that the drainage culvert will failure at the age of 65 years old.

5.3. Performance assessment of the drainage culverts

Based on the Fig. 10 and Fig. 14, Fig. 15 shows the relationship between the mean FOS calculated based on the design code method

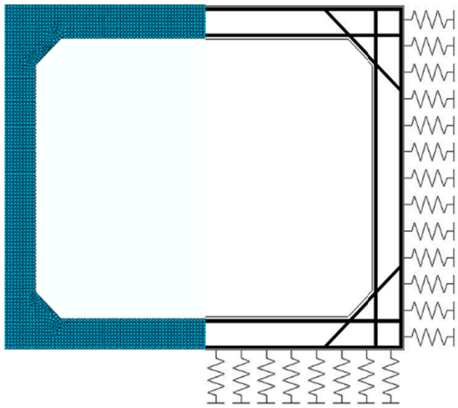

Fig. 11. Mesh and boundary condition of the FEM model.

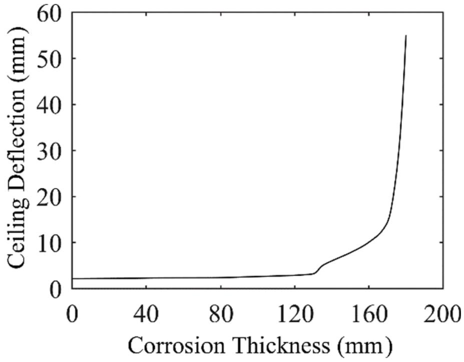

Fig. 12. Relationship between deflection and corrosion thickness.

Fig. 13. Strain diagram of the destroyed drainage culvert.

and service time as well as the relationship between the mean deflection at the mod-span of the roof calculated through the FEM model and service time. Two critical points can be observed from the curves in Fig. 15, i.e., the point at which the mean FOS drops to 1.0 based on the design code method, and the point beyond which the mean deflection of the drainage culvert increases rapidly based on the FEM model. Based on the two points, the service time of the drainage culverts can be divided into three zones, i.e., the safety zone, the critical zone, and the failure zone, as shown in Fig. 15 respectively. Drainage culverts in the safety zone still meet the capacity requirement of the specification and can work normally. Drainage culverts in the critical zone won't break down under normal service load, although the capacity is not enough in accordance with the code. It can be used as a temporary structure under appropriate monitoring and maintenance. Drainage culverts in the failure zone have been unable to bear the normal service load and will collapse at any time, so they need to be repaired or replaced in time. As mentioned previously, the current age of the drainage culvert is about 37 years. Therefore, the drainage culvert of the Nangan line is at the critical zone and it needs to be carefully monitored.

Fig. 16 shows the relationship between failure probability and service time calculated based on the FOS and FEM results. It can be seen that compared with the curve based on FOS, the curve calculated through FEM model has moved back by 25–30 years on the whole, which is in good agreement with the duration of the critical zone in Fig. 15. If we regard the failure probability of 1% as the

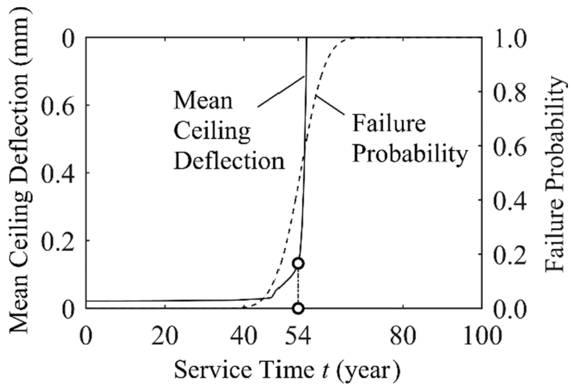

Fig. 14. Relationship of mean ceiling deflection and failure probability with time.

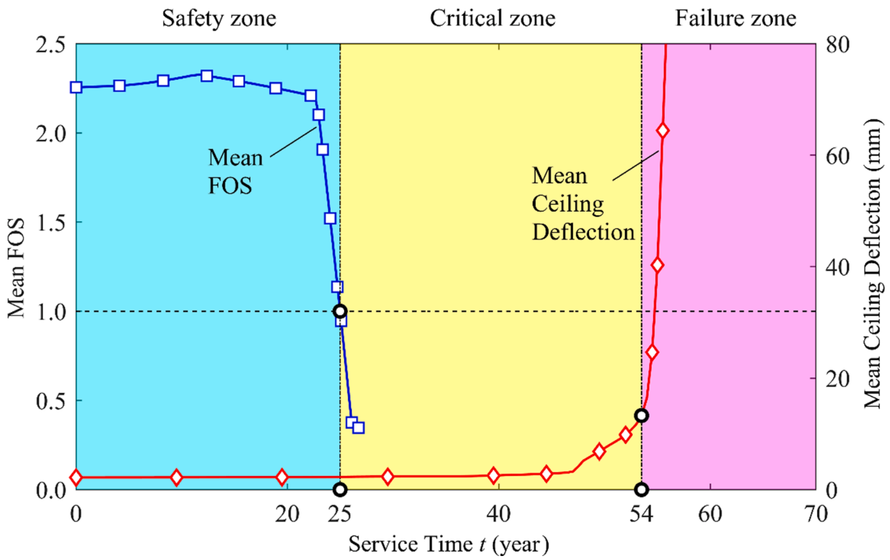

Fig. 15. The whole life cycle of the drainage culvert.

allowable value, the service time of the drainage culverts can also be divided into three zones. Compared with Fig. 15, these three zones shifted to the left for 12 years. In this figure, the drainage culvert of the Nangan line is still at the critical zone, but in five years, it will enter the failure zone. Therefore, the service condition of deteriorating drainage culverts in highly corrosive service environment is more severe considering the uncertainties.

6. Summary and conclusions

The research work reported in this paper and the conclusions obtained are as follows.

(1) The field investigation results regarding the Nangan line are introduced. For the roof of the drainage culverts, it is found that quite some longitudinal bars disappeared, and the thickness of the corroded concrete was generally between 40 and 90 mm. Through the field investigation, it is found that while the ceiling is seriously eroded, the structure under the water is almost intact.
(2) A Gamma process model is used to model the deterioration of the drainage culvert, which is calibrated based on data obtained from the field investigations. Based on the calibrated model, it is found that the corrosion thickness is almost zero in the first few years of service, and the corrosion rate increases with time. When the service time is 32 years, the mean value of corrosion thickness is 60 mm.
(3) When the design code method is used to assess the performance of the drainage culvert, it is found that the mean FOS of the culvert decreases from 2.25 to 1.0 when the cross-sectional area of steel bars decreases from its initial value to half (with the corrosion thickness of 36 mm), where the corresponding service time is 25 years. Taking the uncertainty into account, the failure probability of the culvert is nearly 100% when the service time is 35 years. The results obtained based on the design code

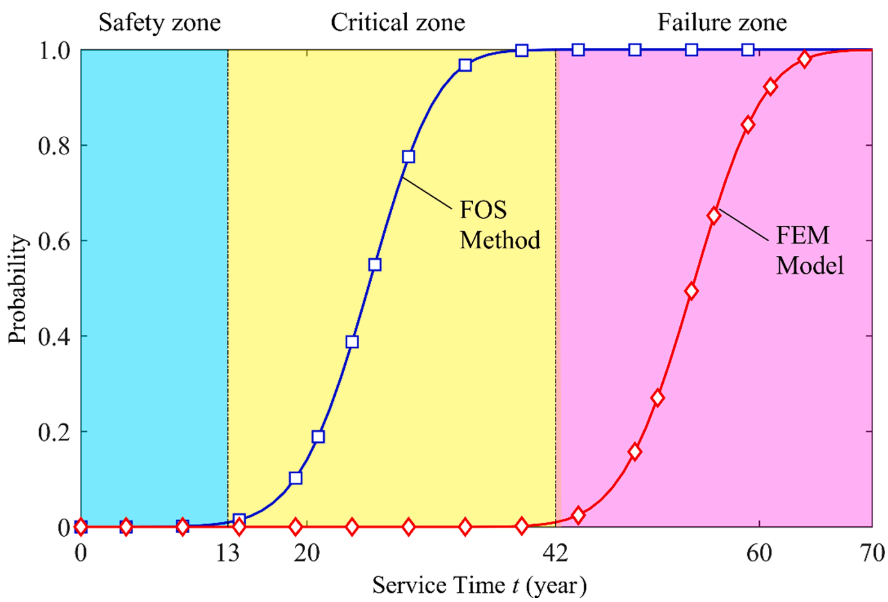

Fig. 16. Relationship between failure probability and service time.

method are contradicts with the actual performance of the drainage culverts due to the conservative assumptions made in the design code method. These assumptions are reasonable in design stage, but seems to be overconservative for ultimate bearing capacity assessment.

(4) To overcome the limitations of the design code method, the performance of the drainage culvert was assessed based on FEM. It is found that the deflection of the roof of the drainage culvert increases rapidly when the corrosion thickness is greater than 170 mm. If we regard the corrosion thickness of 170 mm as the allowable deflection, the service life is about 54 years. Take the uncertainty into account, the failure probability of the structure is less than 1% during the first 42 years of service.

(5) The service time of the drainage culverts can be divided into three zones, i.e., the safety zone, the critical zone, and the failure zone. Safety zone means the drainage culverts can work normally, critical zone means it can be used as a temporary structure under appropriate monitoring and maintenance, and failure zone means it needs to be repaired or replaced in time in the failure zone. The drainage culvert of the Nangan line is at the critical zone and it needs to be carefully monitored.

Declaration of Competing Interest

The authors declare that they have no known competing financial interests or personal relationships that could have appeared to influence the work reported in this paper.

Acknowledgements

This work is supported in part by the National Natural Science Foundation of China (NSFC 51778473) and Shanghai Science and Technology Committee (16DZ1200500).

Appendix 1. Supplementary notes of the selection of calculation parameters and load combination in Table 2

(1) Earth pressure. The soil parameters are weighted average of the soil layers, and the unit weight is 18.3 kN/m^3. C_d is the amplification coefficient of vertical soil pressure on trenched pipes, and $C_d = 1.2$ in conformity with the specification.

(2) Groundwater pressure. The water pressure and soil pressure on the sidewall are calculated separately, and those on the roof are summed together. The bottom water pressure is taken as a part of the foundation reaction and not calculated additionally.

(3) Foundation reaction. It is stated in the specification that when the net width of the rectangular pipe is no more than 3.0m, the foundation reaction is uniformly distributed, as P_{bv} in Fig. 7.

(4) Water pressure inside. The vertical water pressure inside the pipe is not taken as a load because the water pressure is directly offset with the uniformly distributed foundation reaction.

(5) Variable loads on the roof. There are two kinds of ground addition loads acting on the drainage culvert in service: ground surcharge Q_m and vehicle load Q_v. The more adverse one is taken as the variable load, and here the value is 10 kPa.

(6) Combination of loads. The load basic combination is used in the calculation.

References

[1] C. Grengg, F. Mittermayr, A. Baldermann, M.E. Boettcher, A. Leis, G. Koraimann, P. Grunert, M. Dietzel, Microbiologically induced concrete corrosion: A case study from a combined sewer network, Cem. Concr. Res. 77 (2015) 16–25, https://doi.org/10.1016/j.cemconres.2015.06.011.
[2] N. Hernandez, N. Caradot, H. Sonnenberg, P. Rouault, A. Torres, Optimizing SVM models as predicting tools for sewer pipes conditions in the two main cities in Colombia for different sewer asset management purposes, Struct. Infrastruct. Eng. 17 (2) (2021) 156–169, https://doi.org/10.1080/15732479.2020.1733029.
[3] A. Firouzi, M. Abdolhosseini, R. Ayazian, Service life prediction of corrosion-affected reinforced concrete columns based on time-dependent reliability analysis, Eng. Fail. Anal. 117 (2020) 104944, https://doi.org/10.1016/j.engfailanal.2020.104944.
[4] K. Morrison, At last, Coxwell sewer repair finished after delays, unforeseen obstacles, and 'a solid three years of work', 2013. http://nationalpost.com/posted-toronto/at-last-coxwell-sewer-repair-finished.
[5] J. Kyeland, MSD says downtown sewer collapse will take weeks to repair, 2017, September 14. http://nationalpost.com/posted-toronto/at-last-coxwell-sewer-repair-finished.
[6] M. Elmasry, A. Hawari, T. Zayed, An economic loss model for failure of sewer pipelines, Struct. Infrastruct. Eng. 14 (10) (2018) 1312–1323, https://doi.org/10.1080/15732479.2018.1433693.
[7] A.H.S. Garmabaki, S. Marklund, A. Thaduri, A. Hedstrom, U. Kumar, Underground pipelines and railway infrastructure - failure consequences and restrictions, Struct. Infrastruct. Eng. 16 (3) (2020) 412–430, https://doi.org/10.1080/15732479.2019.1666885.
[8] J. Herisson, E.D. van Hullebusch, M. Moletta-Denat, P. Taquet, T. Chaussadent, Toward an accelerated biodeterioration test to understand the behavior of Portland and calcium aluminate cementitious materials in sewer networks, Int. Biodeterior. Biodegrad. 84 (2013) 236–243, https://doi.org/10.1016/j.ibiod.2012.03.007.
[9] G. Jiang, J. Keller, P.L. Bond, Determining the long-term effects of H2S concentration, relative humidity and air temperature on concrete sewer corrosion, Water Res. 65 (2014) 157–169, https://doi.org/10.1016/j.watres.2014.07.026.
[10] C.D. Parker, The corrosion of concrete, Aust. J. Exp. Biol. Med. Sci. 23 (2) (1945) 81–90.
[11] L. Zhang, P. De Schryver, B. De Gusseme, W. De Muynck, N. Boon, W. Verstraete, Chemical and biological technologies for hydrogen sulfide emission control in sewer systems: a review, Water Res. 42 (1–2) (2008) 1–12, https://doi.org/10.1016/j.watres.2007.07.013.
[12] T.A. El Maaddawy, K.A. Soudki, Effectiveness of impressed current technique to simulate corrosion of steel reinforcement in concrete, J. Mate. Civ. Eng. 15 (1) (2003) 41–47, https://doi.org/10.1061/(asce)0899-1561(2003)15:1(41).
[13] EPTA (Environmental Protection Agency Technology), Process design manual for sulfide control in sanitary sewerage systems, Environmental Protection Agency, 1974.
[14] T. Wells, R.E. Melchers, Modelling concrete deterioration in sewers using theory and field observations, Cem. Concr. Res. 77 (2015) 82–96, https://doi.org/10.1016/j.cemconres.2015.07.003.
[15] Y. Bao, D. Feng, N. Ma, H. Zhu, T. Rabczuk, Experimental and numerical study on structural performance of reinforced concrete box sewer with localized extreme defect, Undergr. Space 3 (2) (2018) 166–179, https://doi.org/10.1016/j.undsp.2018.04.001.
[16] R.D. Pomeroy, The Problem of Hydrogen Sulphide in Sewers, Clay Pipe Development Association, London, U.K., 1976.
[17] Q. Ai, Y. Yuan, S.-L. Shen, H. Wang, X. Huang, Investigation on inspection scheduling for the maintenance of tunnel with different degradation modes, Tunn. Undergr. Space Technol. 106 (2020) 103589, https://doi.org/10.1016/j.tust.2020.103589.
[18] J.M. van Noortwijk, J.A.M. van der Weide, M.J. Kallen, M.D. Pandey, Gamma processes and peaks-over-threshold distributions for time-dependent reliability, Reliab. Eng. Syst. Saf. 92 (12) (2007) 1651–1658, https://doi.org/10.1016/j.ress.2006.11.003.
[19] A. Strauss, R. Wan-Wendner, A. Vidovic, I. Zambon, Q. Yu, D.M. Frangopol, K. Bergmeister, Gamma prediction models for long-term creep deformations of prestressed concrete bridges, J. Civ. Eng. Manag. 23 (6) (2017) 681–698, https://doi.org/10.3846/13923730.2017.1335652.
[20] R. Edirisinghe, S. Setunge, G. Zhang, Application of Gamma Process for Building Deterioration Prediction, J. Performance Construct. Facilities 27 (6) (2013) 763–773, https://doi.org/10.1061/(asce)cf.1943-5509.0000358.
[21] B.R. Ellingwood, Y. Mori, Probabilistic methods for condition assessment and life prediction of concrete structures in nuclear-power-plants, Nucl. Eng. Des. 142 (2–3) (1993) 155–166, https://doi.org/10.1016/0029-5493(93)90199-j.
[22] Q.-Q. Wen, M.-C. Chen, Study on the nonlinear performance degradation of reinforced concrete beam under chloride ion corrosion, Eng. Fail. Anal. 124 (2021) 105310, https://doi.org/10.1016/j.engfailanal.2021.105310.
[23] H. Zhou, S. Chen, Y. Du, Z. Lin, X. Liang, J. Liu, F. Xing, Field test of a reinforced concrete bridge under marine environmental corrosion, Eng. Fail. Anal. 115 (2020) 104669, https://doi.org/10.1016/j.engfailanal.2020.104669.
[24] CECS (China Association for Engineering Construction Standardization), Specification for structural design of buride rectangular pipeline of water supply and Sewerage engineering, CECS 145: 2002, CECS, Beijing, China, 2002.
[25] MOHURD (Ministry of Housing and Urban-Rural Development of the People's Republic of China), Code for design of concrete structures, GB50010-2010, China Architecture & Building Press, Beijing, China, 2010.
[26] A.H.S. Ang, W.H. Tang, Probability concepts in engineering planning and design: Emphasis on application to civil and environmental engineering, Wiley, New York, 2007.
[27] DSSC (Dassault Systemes Simulia Corp), Abaqus Theory Manual, version 6.14, Dassault Systemes Simulia Corp, Providence,RI,USA, 2014.
[28] J. Jiang, Finite element techniques for static analysis of structures in reinforced concrete, Chalmers University of Technology, Sweden, 1983.
[29] Y. Tang, Y. Cai, D. Feng, Full-scale Experiment and Ultimate Bearing Capacity Assessment of Reinforced Concrete Drainage Culverts with Defects, KSCE J. Civ. Eng. 25 (11) (2021) 4348–4358, https://doi.org/10.1007/s12205-021-5270-5.
[30] J. Lubliner, J. Oliver, S. Oller, E. Oñate, A plastic-damage model for concrete, Int. J. Solids Struct. 25 (3) (1989) 299–326, https://doi.org/10.1016/0020-7683(89)90050-4.
[31] J.H. Lee, G.L. Fenves, Plastic-damage model for cyclic loading of concrete structures, J. Eng. Mech. 124 (8) (1998) 892–900, https://doi.org/10.1061/(asce)0733-9399(1998)124:8(892).
[32] V. Birtel, P. Mark, Numerical analyses of the biaxial shear capacity of transverse reinforced concrete members, in: 8th International Conference on Computational Structures Technology, Stirling, 2006.
[33] D.A. Hordijk, Tensile and tensile fatigue behaviour of concrete; experiments, modelling and analyses, Heron 37 (1) (1992) 1–79.
[34] J. Yuan, X. Lou, X. Yao. Design principle of foundation engineering, China Constructions Press, Beijing, 2011.
[35] T. Rabczuk, J. Akkermann, J. Eibl, A numerical model for reinforced concrete structures, Int. J. Solids Struct. 42 (5–6) (2005) 1327–1354, https://doi.org/10.1016/j.ijsolstr.2004.07.019.